Digest Journal of Nanomaterials and Biostructures Vol. 6, No 4, October-December 2011, p. 1983-1990

THE MORPHO-STRUCTURAL CHARACTERISTICS OF TiO_2 PHOTOELECTRODES PREPARED BY ADVANCED LASER DEPOSITION FOR DYE SENSITIZED SOLAR CELLS APPLICATIONS

C. SIMA[a,b], C. GRIGORIU[a*], C. TAZLAOANU[b], S. ANTOHE[b]
[a]*National Institute for Laser, Plasma and Radiation Physics, Laser department, 409 Atomistilor street, P.O. Box MG-36, 077125, Bucharest-Magurele, Romania*
[b]*University of Bucharest, Faculty of Physics, 405 Atomistilor street, P. O. Box MG-11, 077125, Bucharest-Magurele, Romania*

Mesoporous TiO_2 photoelectrodes using picosecond lasers (8 ps) with a high repetition rate (50 kHz) and low energy/pulse (20 μJ) were successfully used in the fabrication of dye-sensitized solar cells (DSSCs). The variation of the morpho-structural characteristics of TiO_2 films deposited on indium tin oxide (ITO) substrates in the presence of different oxygen pressures (0.04-1 Torr) was investigated. The oxygen pressure had a significant influence on the film crystallinity, porosity and adherence, and as a result, on the cell global efficiency. In the specific experimental conditions (532 nm laser wavelength, 0.17 J/cm^2 fluence, 0.3 Torr oxygen pressure, 450 ^{0}C annealed film), a TiO_2 phase mixture of rutile/anatase (85/15), with a grain size of 17.8 nm, was sintered. Using these films as photoelectrodes, solar cells illuminated with AM 1.5 (100 mW/cm^2) provided a maximum power of 1.56 mW/cm^2 and an integral power conversion efficiency of 1.81%.

(Received November 17; accepted December 20, 2011)

Keywords: TiO_2, laser ablation, Solar cell, DSSCs

1. Introduction

The need for renewable energy resources has driven research in the field of solar cells. DSSCs are potential candidates for solar energy due to low-cost production, high-energy conversion efficiency (~11%) and transparency.

Since 1991, DSSCs based on dye-sensitized porous nanocrystalline titanium dioxide photoelectrodes have been extensively researched by the academic and industrial community [1-7].

Nanocrystalline TiO_2 film is a basic component of DSSCs. A large variety of TiO_2 film fabrication procedures can be found in the literature. The most common methods are doctor-blading and screen printing, which begin with a mixture of TiO_2 nanoparticles and organic additives. These methods have some drawbacks. TiO_2 photoelectrode fabrication requires an additional high temperature process (~ 450 ^{0}C) to remove the organic additives, which implies extra cost and environmental effects. Moreover, the shrinkage resulting from the decomposition of the organic additives produces cracks, especially when the film is thicker (5-15 μm).

Other fabrication methods have been also developed for deposition of TiO_2 such as magnetron sputtering [6-9], chemical vapor deposition [10, 11], electron beam evaporation [4], electrophoresis [5].

Progress in laser coating technology has provided new possibilities for film sintering. Deposition of thin films by laser ablation (pulsed laser deposition, PLD) has been continuously developed, and a great variety of materials have been synthesized, among them, TiO_2. The TiO_2 photoelectrodes made by pulsed laser deposition offer more advantages:

* Corresponding author: grigoriu@ifin.nipne.ro

(a) it is not necessary to use organic additives (binders and dispersants) as in conventional photoelectrode sintering methods; (b) crack-free thick films can be sintered without difficulty; and (c) the TiO_2 film thickness can be easily and precisely controlled.

Generally, conventional PLD uses high power pulsed lasers with a high energy/pulse (×mJ-×100 mJ) and relatively low repetition rates (×Hz-×100 Hz). The TiO_2 films grown by this technique have micron-sized particulates in or on the film, are compact and often show columnar growth. From the point of view of DSSCs, a compact TiO_2 film is disadvantageous because without pores the penetration of the dye in the TiO_2 film is insignificant. Therefore, conventional PLD is not suitable for the synthesis of solar cell TiO_2 photoelectrodes. In fact, the large majority of the papers on TiO_2 films grown by conventional PLD [12-18] deal with film synthesis and characteristics but do not demonstrate their efficiency as TiO_2 photoelectrodes in DSSCs .

There are very few reports on TiO_2 films produced by conventional PLD and used in DSSCs [19, 20]. For example, standard PLD with a nanosecond excimer laser was used in [19] for the deposition of very thin (30 nm) TiO_2 films, but only for use as electrical isolators; afterward, a mesoporous TiO_2 layer was deposited by laser-induced forward transfer, starting from a colloidal TiO_2 paste.

The development of high repetition rate (×kHz-×MHz) ultrafast lasers with low energy/pulse (×μJ) offered new opportunities for laser deposition technology. The availability of advanced high repetition picosecond or femtosecond lasers led to significant changes in the ablation process and, therefore, in the structure of the deposited films [21]. In this case, the film is formed by ablation from the target of a very small quantity of material, inhibiting the ablation of micron-sized droplets; on the other hand, due to the high repetition rate, a continuous flow of nanoparticles is possible. In this way, such systems allow a fine control over the quality of the film.

This is why we considered this technique for the fabrication of TiO_2 films, with a final application as photoelectrodes in DSSCs. To the best of our knowledge, this is the first demonstration of this method for the synthesis of DSSC TiO_2 photoelectrodes.

In this article, we present the characteristics of mesoporous titania films grown by PLD using a high repetition rate, low energy/pulse, picosecond laser. The influence of the sintering conditions on the effectiveness of the photoelectrode was studied, and DSSC performances are presented.

2. Experimental

The dye-sensitized solar cells studied in this work had a standard structure. The TiO_2 photoelectrode was prepared by PLD using a picosecond Nd:YVO_4 laser (8 ps pulse duration, 532 nm wavelength, 1 W average power, 5×10^4 pps pulse repetition rate, 0.17 J/cm^2 fluence). As target, titanium (99.9%) was used; the substrate-target distance was 3 cm. The deposition was performed in an oxygen atmosphere at different pressures in the range of 0.04 -1 Torr. In order to have good electrical contact between the TiO_2 particles, after deposition the TiO_2 films were subjected to thermal treatment at 450 ^{0}C for two hours in an oxygen atmosphere.

After cooling to 90 ^{0}C, the photoelectrodes were stained by immersion in a solution of Ruthenium 535 dye (Solaronix) for 12 hours.

The substrate was ITO deposited on glass (Kintec, 25 mm × 25 mm, with 18 ohm/sq resistivity). The resistivity increased to 52 ohm/sq after thermal treatment at 450 ^{0}C.

The platinum-coated conducting glass was used as a counter electrode (from Solaronix, with ~14.5 Ω/sq resistivity). For easily electrolyte filling, two holes (1 mm diameter) were drilled.

The two electrodes were assembled by means of a thermoplastic sealing gasket, 60 μm in thickness, heated to 120 ^{0}C. The cell was filled with the electrolyte iodolyte AN50 (Solaronix). The two holes were sealed with the same thermoplastic membrane.

The morpho-structural analyses were performed by scanning electron microscopy (SEM) with a Quanta Inspect F microscope and X ray diffraction (XRD) with a Ital-Structures model GNR APD2000 diffractometer.

In order to evaluate the global efficiency, the cells were irradiated with a 100 mW/cm^2, lamp model OSRAM 600 W with a 1.5 AM filter. The device illumination was made through a

mask of 10×10 mm^2 in order to avoid any additional light, which could be transmitted by the glass edges or reflections from the silver paint. The current-voltage (I-V) characteristics were recorded by a Keithley 6517 A electrometer and a Keithley 2400 sourcemeter.

3. Results and discussion

The morpho-structural characteristics of the TiO_2 films deposited at different oxygen pressures are presented below.

XRD spectra of the films deposited at oxygen pressure of 1-0.04 Torr at room temperature (RT) and annealed at 450 ^{0}C are plotted in figures 1-3.

In figure 1 (a) and (b), it is evident that the films deposited at 1 Torr oxygen pressure present characteristic peaks of the TiO_2 rutile phase and ITO (used as the substrate). The TiO_2 films deposited at RT exhibit only an incipient rutile phase superposed on an amorphous background. After the thermal treatment, the film was very well crystallized, and an additional Ti_3O peak appeared. The grains size evaluated from XRD spectra using the Debye-Scherer formula was 18.2 nm.

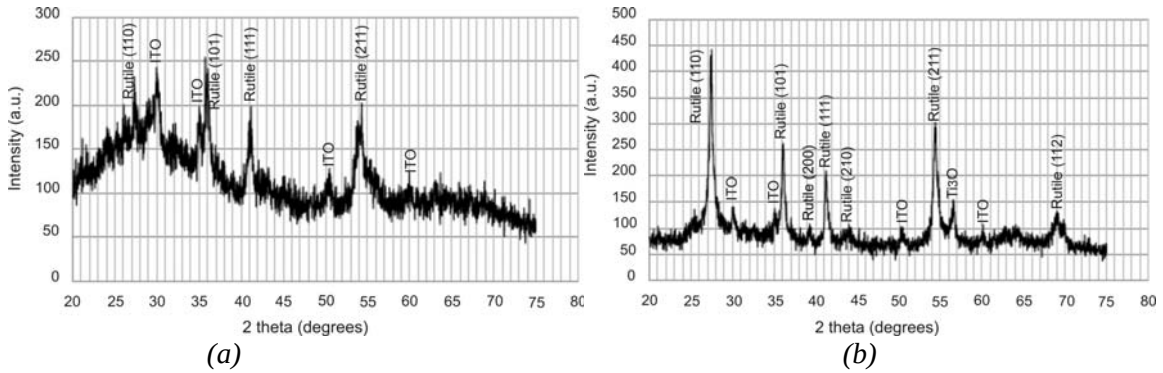

Fig.1 XRD spectra of the TiO_2 films deposited at 1 Torr oxygen pressure: a) RT, b) annealed at 450 ^{0}C.

In figure 2 (a) and (b) XRD spectra are presented for the films deposited at 0.3 Torr. In this case, in addition to the rutile phase, an incipient anatase phase appeared (fig. 2a) at RT. After annealing, the films became better crystallized, but a mixture of anatase and rutile phases formed (fig. 2b): 15% anatase and 85% rutile. The grain size was 17.8 nm.

We must mention that also at 0.5 Torr, the film exhibited similar XRD spectra as at 0.3 Torr.

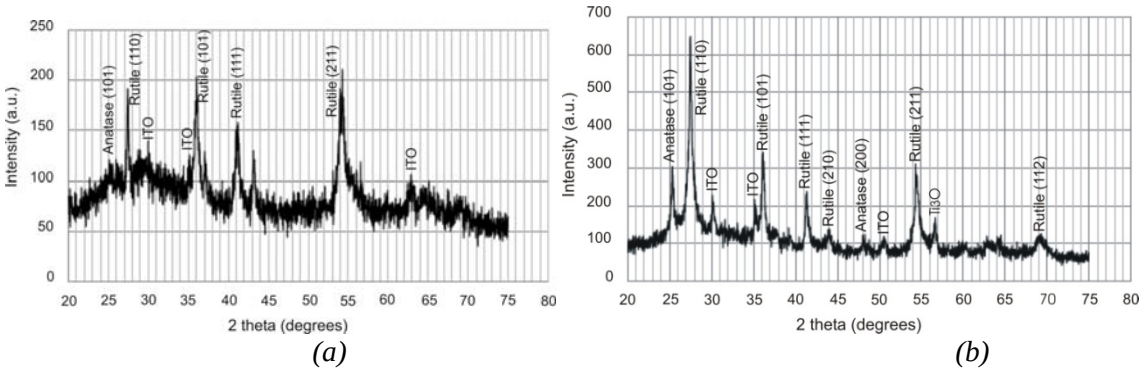

Fig. 2 XRD spectra of the films deposited at 0.3 Torr oxygen pressure:a) RT, b) annealed at 450 ^{0}C.

The films deposited at 0.04 Torr oxygen pressure, fig. 3 (a) and (b) show that at RT no rutile phase formed, but only the peak characteristic of the anatase phase (112) was observed. After thermal treatment, anatase and rutile phases appeared;

quantitative analysis indicated a mixture of approximately 28% anatase and 72% rutile with 18 nm grain size.

The XRD results indicated that the thermal treatment was critical for film crystallization.

On the other hand, the phase composition also was dependent on the oxygen pressure. At higher pressures, the rutile phase was more dominant.

At higher oxygen pressures (concentration), the rutile phase was promoted than anatase because in the laser beam-target interaction region, the temperature was higher due to the oxidation reaction, and at higher temperatures, rutile phase was formed.

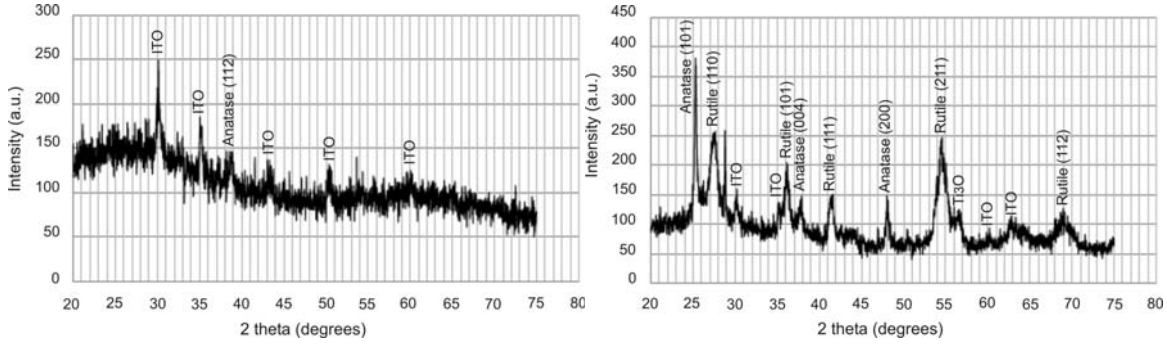

(a) *(b)*

Fig.3 XRD spectra of the films deposited at 0.04 Torr oxygen pressure: a) RT, b) annealed at 450 ^{0}C.

One of the factors which determines the performance of the cells is specific surface area and film porosity because it is needed for TiO_2 photoelectrode dye impregnation. Therefore, we were interested in the film structure, particularly after thermal treatment (as the films were to be utilized as photoelectrodes in DSSCs).

In figure 4, the SEM images of the films deposited at RT and different oxygen pressures are presented after thermal treatment.

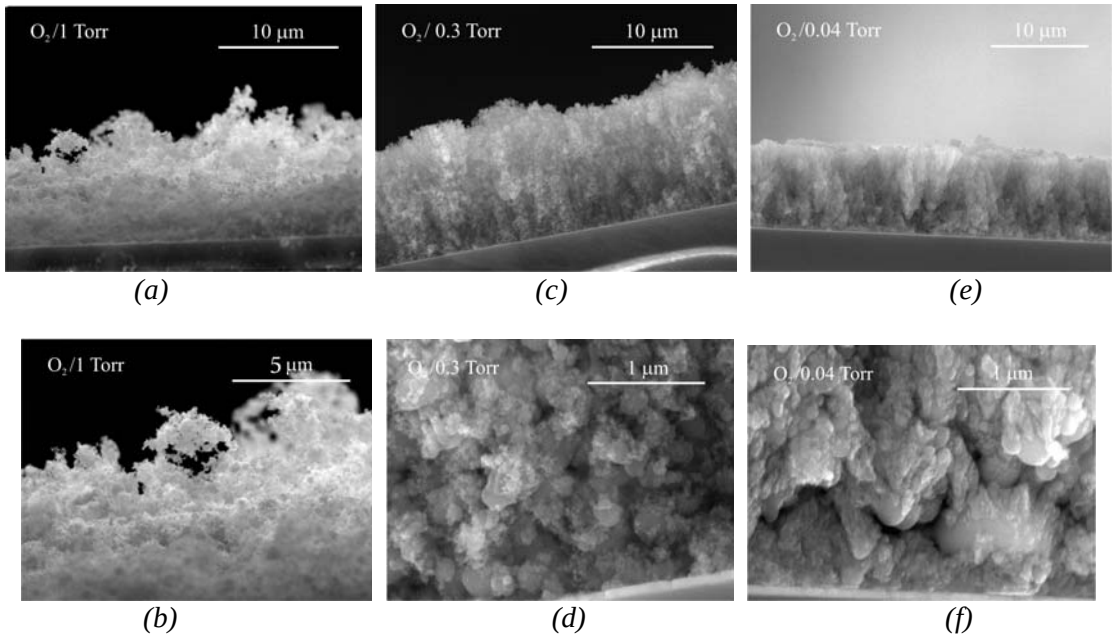

(a) *(c)* *(e)*

(b) *(d)* *(f)*

Fig. 4 SEM cross section images of the films deposited at different oxygen pressures and RT; after deposition the films were annealed at 450 ^{0}C.

The investigations show that at higher deposition pressure the films became more porous, but at the same time the adherence on the ITO/glass substrate decreased despite the thermal treatment. The films deposited at 1 and 0.3 Torr (fig. 4(a)-(d)) had a porous structure consisting of nanometric particle agglomerations.

At 1 Torr, it was obvious that the film had larger pores. At higher pressure, the collision rate of the ejected nanoparticles with oxygen molecules is higher, leading to larger agglomerations. On the other hand, due to the fact that the velocity of the agglomerated particulates toward the substrate decreased significantly at 1 Torr, their adherence to the substrate and to other agglomerations was weaker. Thus, films deposited at an oxygen pressure of 1 Torr had practically no adherence and were easily wiped away. In addition, the particle packing density decreased, and the pores became larger.

On the other hand, if the pressure was decreased drastically to 0.04 Torr (fig. 4 (e),(f)), a major change in the film structure was observed. These films were compact, showed columnar growth and had much lower porosity and very good adherence. The lower porosity of the films deposited at low pressure was also confirmed by the fact that after the dye impregnation, the color of the film was much more pale in comparison with the films grown at higher pressures.

Taking into account the above facts, from morphological point of view, the most suitable films were those fabricated at 0.3 Torr.

We must also mention another advantage of the method used in this work: all films regardless the deposition pressures are crack free. This feature is very important; the films deposited by the standard "doctor blade" method, for example, have some drawbacks. If the film is thicker (> 5 μm), it is difficult to avoid the cracks.

The performances of the solar cells based on the TiO_2 films described above are presented below.

Fig. 5 shows plots I-V characteristics in the fourth quadrant (a) and power-voltage (P-V) (b) curves for a cell fabricated with the TiO_2 film deposited at 0.3 Torr and annealed at 450 ^{0}C (film thickness: 13 μm) illuminated by an integrated power of 100 mW/cm^2. The typical cell parameters were a maximum output power P_{max}= 1.56 mW/cm^2, a short-circuit current I_{sc}=3.72 mA/cm^2, an open-circuit voltage V_{oc}=767 mV, and a fill factor FF=0.61.

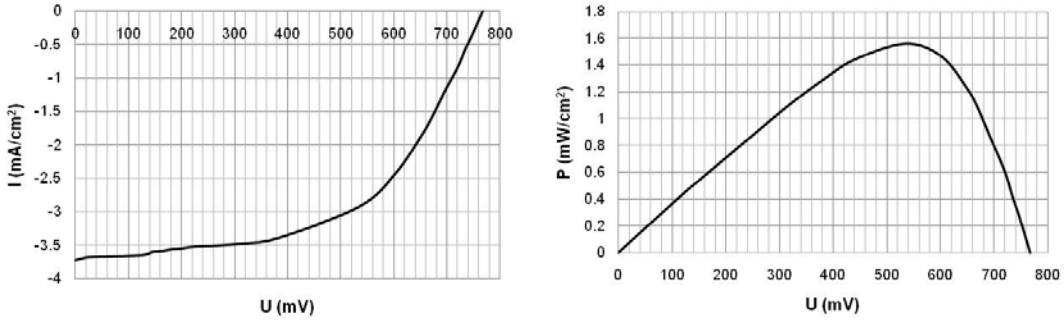

(a) *(b)*

Fig. 5 I-V (a) and P-V (b) characteristics of the cell with a TiO_2 photoelectrode sintered at 0.3 Torr, 450 ^{0}C, film thickness: 13 μm.

The estimation of the series and shunt resistances of the cell were based on I-V characteristics. The equivalent circuit of the cell deposited at 0.3 Torr is drawn in fig. 6. From calculation, the value of the series resistance is 58 Ω, and the shunt resistance is 2.6 kΩ.

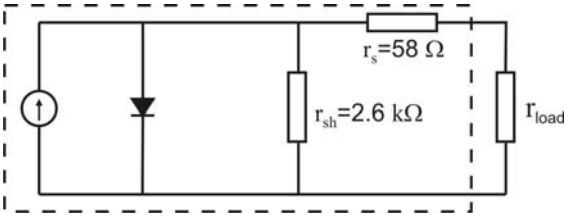

Fig. 6 Equivalent circuit of the cell obtained using a TiO_2 film deposited at 0.3 Torr.

It is clear that the poor efficiency of the cell was in principal due to the low amount of absorbed dye and low diffusivity of the iodine species. Presence of the rutile phase and high series resistance, are also responsible for additional losses. In our case, ITO had an initial resistivity of 18 ohm/sq, but it increased to 52 ohm/sq after thermal treatment at 450 ^{0}C.

Table 1 summarizes the main characteristics of the solar cells with photoelectrodes prepared at different oxygen pressures.

Table 1. Characteristics of the cells using TiO_2 photoelectrodes obtained directly by laser ablation.

Cell no.	Oxygen pressure (Torr)	TiO_2 film thickness (μm)	T (^{0}C)	V_{oc} (mV)	I_{sc} (mA/cm^2)	P_{max} (mW/cm^2)	η(%) Without tacking into account reflection *	η(%) Tacking into account reflection*
1	1	11.4	450	532	0.32	0.09	0.09	0.10
2	0.5	13.4	450	730	1.66	0.6	0.6	0.69
3	0.3	8.3	450	723	4.16	1.5	1.5	1.74
4	0.3	13.0	450	767	3.72	1.56	1.56	1.81
5	0.3	8.0	RT	488	0.83	0.14	0.14	0.16
6	0.04	5.7	450	348	0.41	0.06	0.06	0.07

(* reflection of the incident light on the cell).

First of all, one can note that the cells prepared at 0.3 Torr and annealed at 450 ^{0}C provided the highest efficiency. The insignificant difference of the efficiency between the cells with film thicknesses of 8.3 and 13 μm (cells 3 and 4) indicated that the optimal thickness of the TiO_2 film is around 10 μm. Comparing the cells with annealed and unannealed films (see cell no 3 and 5), the efficiency decreased dramatically for those that were not annealed. This result can be explained by the poor crystallinity and low electrical connectivity of the particles, which cannot ensure a high mobility of the photocharge carriers and good collection.

In the case when the film was deposited at higher pressure, the efficiency diminished considerably to 0.69% or 0.1% for the 0.5 or 1 Torr deposition oxygen pressures, respectively. This is caused by low particle connectivity in terms of the particle packing density. Because the particles or clusters ejected from the target slow down considerably at higher pressures, the film had a lower packing density, larger pores and consequently a lower interparticle connectivity. In addition, as XRD investigation (fig. 1) showed, at higher pressures the film structure presented only the rutile phase; this contributed to the decrease in the cell performance because the electron transport is slower in the rutile layer than in the anatase layer [22].

In addition, the cells deposited at very low pressure, 0.04 Torr, were very poor, but the explanation is different. As we mentioned above, in this case, the TiO_2 electrode was a very dense layer with very low porosity (figures 4 (e),(f)), which does not allow the dye absorption in the

TiO_2 film (also demonstrated by the film faint color after dye impregnation). This decreased the photoactive area responsible for the photovoltaic response.

4. Conclusions

Laser ablation method for directly producing TiO_2 photoelectrodes using high repetition rate (50 kHz) and ultrafast lasers (8 ps) with a low energy/pulse (20 μJ) was successfully demonstrated.

We underline that the nanoporous crack-free films can be sintered without difficulty, regardless of the film thickness, without the need for organic additives. The study indicated an optimal oxygen pressure of 0.3 Torr at which the film was nanoporous and crack-free, consisting of a rutile/anatase mixture with a 17.8 nm grain size.

The maximum power and conversion efficiency were 1.56 mW/cm^2 and 1.81%, respectively.

Despite the fact that the cell efficiency was still lower in comparison with those fabricated by conventional methods, new possibilities are opened. This method is expected to be further improved by additional relevant experiments under carefully tailored conditions (laser wavelength, repetition rate, fluence, etc., high specific surface area and obtaining of anatase phase).

Acknowledgements

This work was supported by a grant (POSDRU/89/1.5/S/58852) from the Romanian Government and the European Social Fund within the Sectorial Operational Program Human Resources Development 2007-2013.

All authors have equal contribution to this work.

References

[1] B. Oregan, M. Grätzel, Nature **353**, 737 (1991).
[2] 3rd International Conference on the Industrialization of Dye Solar Cells (DSC-IC 09), April 22 - 24, 2009, Nara, Japan, http://www.dsc-ic.com.
[3] C. Sima, C. Grigoriu, S. Antohe, Thin Solid Films **519**, 595 (2010).
[4] M. Manca, F. Malara, L. Martiradonna, L. Marco, R. Giannuzzi, R. Cingolani, G. Gigli, Thin Solid Film **518**, 7147 (2010).
[5] H. Chang, H. Su, W. Chen, K. Huang, S. Chien, S. Chen, C. Chen, Sol. Energy **84**, 130 (2010).
[6] M. Hossain, S. Biswas, T. Takahashi, Y. Kubota, A. Fujishima, Thin Solid Films **516**, 7149 (2008).
[7] V.Senthilkumar, M. Jayachandran, C. Sanjeeviraja, Thin Solid Films **519**, 991 (2010).
[8] M. Khadar, N. Shanid, Surf. Coat. Tech **204**, 1366 (2010).
[9] D. Ren, Y. Zou, C. Zhan, N. Huang, J. Korean Phys. Soc, **58**, 883 (2011).
[10] P. Shinde, C. Bhosale, J. Anal. Appl. Pyrolysis **82**, 83 (2008).
[11] C. Quinonez, W. Vallejo, G. Gordillo, Appl. Surf. Sci **256**, 4065 (2010).
[12] M. Walczak, E. Papadopoulou, M. Sanz, A. Manousaki, J. Marco, M. Castillejo, Appl. Surf. Sci. **255**, 5267 (2009).
[13] H. Long, G. Yang, A. Chen, Y. Li, P. Lu, Thin Solid Films **517**, 745 (2008).
[14] C. Sima, C. Grigoriu, Thin Solid Films **518**, 1314 (2009).
[15] Y. Xu, M. Shen, Appl. Phys. A **94**, 275 (2009).
[16] M. Walczak, M. Oujja, J. Marco, M. Sanz, M. Castillejo, Appl. Phys. A **93**, 735 (2008).
[17] M. Sanz, M. Walczak, M. Oujja, A. Cuesta, M. Castillejo, Thin Solid Films **517**, 6546 (2009).
[18] M. Sanz, M. Walczak, R. Nalda, M. Oujja, J. Marco, J. Rodriguez, J. Izquierdo, L. Banares, M. Castillejo, Appl. Surf. Sci. **255**, 5206 (2009).

[19] H. Kim, G. P. Kushto,C. B. Arnold, Z. H. Kafafi, A. Pique, Appl. Phys. Letters **85**, 464 (2004).
[20] H. Kim, R,C.Y. Auyeung, M. Ollinger, G. P. Kushto, Z. H. Kafafi, A. Pique, Appl. Phys. A, **83**, 73 (2006).
[21] E. G. Gamaly, A. V. Rode, B. Luther-Davies, J. Appl. Phys. **85**, 4213 (1999).
[22] N. G. Park, J. van de Lagemaat, A. J. Frank, J. Phys. Chem. B, **104**, 8989 (2000).